2,7-Diaminobenzopyrylium Dyes Are Live-Cell Mitochondrial Stains

Sambashiva Banala, Ariana N. Tkachuk, Ronak Patel, Pratik Kumar, Timothy A. Brown, and Luke D. Lavis*

ACCESS | Metrics & More | Article Recommendations | Supporting Information

ABSTRACT: Small-molecule fluorescent stains enable the imaging of cellular structures without the need for genetic manipulation. Here, we introduce 2,7-diaminobenzopyrylium (DAB) dyes as live-cell mitochondrial stains excited with violet light. This amalgam of the coumarin and rhodamine fluorophore structures yields dyes with high photostability and tunable spectral properties.
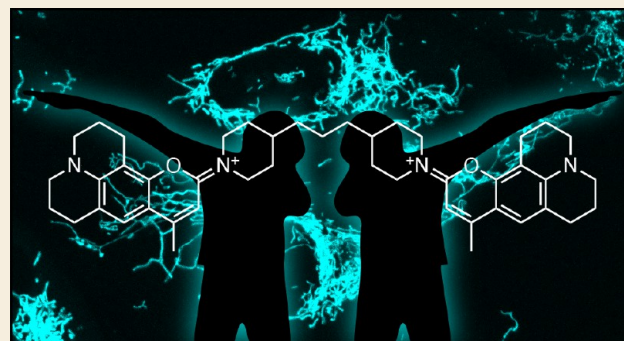
INTRODUCTION

Fluorescence microscopy is an essential tool to interrogate biological structure. A key element in any imaging experiment is the labeling strategy used to localize a fluorophore to the cellular component of interest.[1−5] In addition to measuring the position and movement of specific biomolecules, cellular imaging experiments often involve the visualization of different organelles to quantify their dynamics[6] or provide useful subcellular reference marks.[7−9] Fusing a fluorescent protein to a targeting motif can allow labeling of cellular organelles but requires expression of an exogenous molecule. Fluorescent reagents with affinities for organelle-specific biomolecules can allow imaging without genetic manipulation but typically involve preparation of a small-molecule fluorophore conjugated to an antibody or drug. An alternative labeling strategy is the use of fluorescent stains that accumulate in specific organelles due to the different chemical environments found in these distinct subcellular regions. Examples include tertiary amine-containing dyes accumulating in acidic lysosomes[10] or hydrophobic fluorophores partitioning into lipid droplets.[11]

A widely used fluorescent staining strategy involves mitochondria, whose double membrane structure reflects their role as the powerhouse of the cell. The proteins that comprise the electron transport chain reside in the inner mitochondrial membrane that separates the matrix from the intermembrane space. Their activity drives protons across the inner membrane, resulting in a large voltage difference between these two compartments. This unique membrane potential drives the accumulation of lipophilic cations into the matrix or inner membrane. This was first observed with Rhodamine 123 (**1**),[12] where esterification of the standard *ortho*-carboxyl group

found in rhodamines endows the molecule with a fixed cationic charge. The strategy was expanded to tetramethylrhodamine methyl ester (TMRM, **2**), yielding a red-shifted mitochondrial stain.[13] This general idea was refined with the development of MitoTracker Orange (**3**), in which the carboxyl ester functionality found in rhodamines **1** and **2** is discarded entirely.[7] Compound **3** also incorporates a chloromethyl moiety to allow formation of a glutathione adduct, thereby trapping the fluorophore inside the cell.[14]

The majority of fluorescent mitochondrial stains are based on rhodamine (e.g., **1**−**3**) and cyanine structures.[7] These dyes exhibit relatively long absorption maxima (λ_{abs}) and fall into the standard blue (488 nm), green-yellow (560 nm), and red (640 nm) excitation windows used in fluorescence imaging. Mitochondrial stains excited with violet light (405 nm) have received less attention since there is no general cationic dye scaffold with an excitation maximum in this wavelength range. We sought, and now report, a new class of mitochondrial stains based on 2,7-diaminobenzopyrylium (DAB) dyes.

RESULTS AND DISCUSSION

To create a violet-excited mitochondrial stain, we first considered coumarin dyes, which remain the most utilized

fluorophores excited by ultraviolet (UV) and violet light. The simplest fluorescent coumarins are 7-hydroxy derivatives such as 4-methylumbelliferone (**4**, Figure 1b). We noted that the
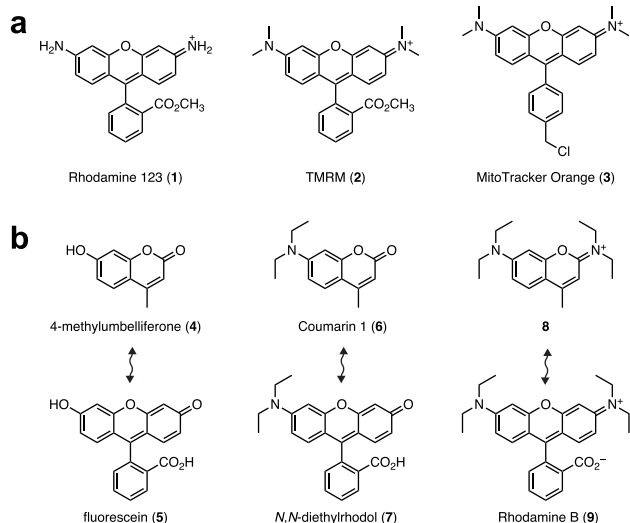

Figure 1. 2,7-Diaminobenzopyrylium (DAB) dyes as potential mitochondrial stains. (a) Chemical structures of mitochondrial stains **1**−**3**. (b) Pairs of structurally consonant dyes: 4-methylumbelliferone (**4**) and fluorescein (**5**); Coumarin 1 (**6**) and *N,N*-diethylrhodol (**7**); 2,7-diaminobenzopyrylium **8** and Rhodamine B (**9**).

classic fluorophore fluorescein (**5**) is effectively the phenylogous derivative of **4**. Similarly, 7-aminocoumarins such as Coumarin 1 (**6**) are structurally consonant with rhodols like **7**. Inspired by the structural relationship between compounds **4**/**5** and **6**/**7**, we considered 2,7-diaminobenzopyrylium (DAB) structures exemplified by the tetraethyl derivative **8**; this is the "coumarin-sized" analog of Rhodamine B (**9**). Although iminocoumarins have received some attention as dyes[15] and indicators,[16] the cationic 2,7-diaminobenzopyrylium fluorophore scaffold is essentially unexplored, with a lone report in the Soviet chemistry literature from 1989.[17]

We began our investigation by synthesizing the known tetraethyl DAB dye **8** starting from Coumarin 1 (**6**, Scheme 1a).[17] Treatment with Et$_3$OBF$_4$ generates a 2-ethoxychromenylium intermediate that reacts with diethylamine to give **8**, which we obtained in 41% yield. Based on the success of this simple synthetic protocol, we prepared additional DAB dyes. We transformed the bright azetidinylcoumarin[18] **10** into the diazetidinyl dye **11** (Scheme 1b). We also explored dyes derived from Coumarin 102 (**12**); reaction with diethylamine, azetidine, or piperidine yielded compounds **13**−**15** (Scheme 1c).

We then evaluated the spectral properties of the DAB dyes **8**, **11**, and **13**−**15** in phosphate-buffered saline (PBS; Table 1, Figure 2a−c) comparing them to the parent coumarin fluorophores **6**, **10**, and **12**. In general, the transformation of the carbonyl group into an iminium moiety elicits a bathochromic shift of ~50 nm in λ_{abs} and a shift of 25−35 nm in fluorescence emission maxima (λ_{em}). Thus, all the DAB dyes exhibit $\lambda_{abs} > 400$ nm, absorbing in the violet-blue region of the visible spectrum. The reduced shift in λ_{em} results in smaller Stokes shifts for the DAB fluorophores relative to the coumarin starting materials. Despite this decrease, the Stokes shifts of the DAB dyes (65−100 nm) remain substantially larger than those of fluoresceins or rhodamines (~25 nm).
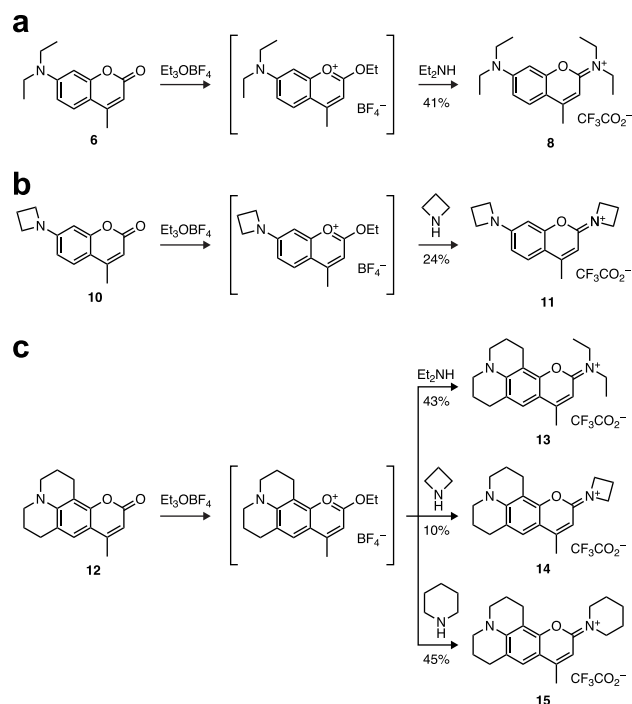
Scheme 1. Synthesis of dyes 8 (a), 11 (b), and 13−15 (c)

Table 1. Spectral Properties of DAB Dyes[a]

scaffold	X	dye	λ_{abs} (nm)	ε (M^{-1}cm^{-1})	λ_{em} (nm)	Φ_f	t_b	N_p
	=O	6	383	23,100	467	0.06	58.1	1310
	=N$^+$	8	428	42,600	493	0.16	85.6	18500
	=O	10	354	15,000	467	0.96	10.3	1490
	=N$^+$	11	402	28,400	501	0.79	19.3	7940
	=O	12	393	20,100	488	0.80	1.81	550
	=N$^+$	13	445	37,200	513	0.75	9.74	9120
	=N$^+$	14	445	39,000	523	0.65	9.91	8430
	=N$^+$	15	446	34,600	522	0.66	9.97	7630

[a]All values measured in PBS, pH 7.4, solution.

Finally, for each matched pair, the DAB congeners show substantially higher photobleaching time constants (t_b) and average number of photons emitted before photobleaching (N_p) relative to the corresponding coumarin dye.

Comparison of specific dye pairs reveal more nuanced differences. The transformation of Coumarin 1 (**6**) to DAB dye **8** yields a shift of 45 nm in λ_{abs} and 26 nm in λ_{em}, resulting in a Stokes shift of 65 nm (Table 1, Figure 2a). Conversion of coumarin **10** into diazetidinyl DAB derivative **11** results in a bathochromic shift of 48 nm in λ_{abs} and a difference of 34 nm in λ_{em} (Table 1, Figure 2b). This larger shift in emission maximum combined with the properties of the parent coumarin **10** gives a Stokes shift of 99 nm for **11**. For DAB
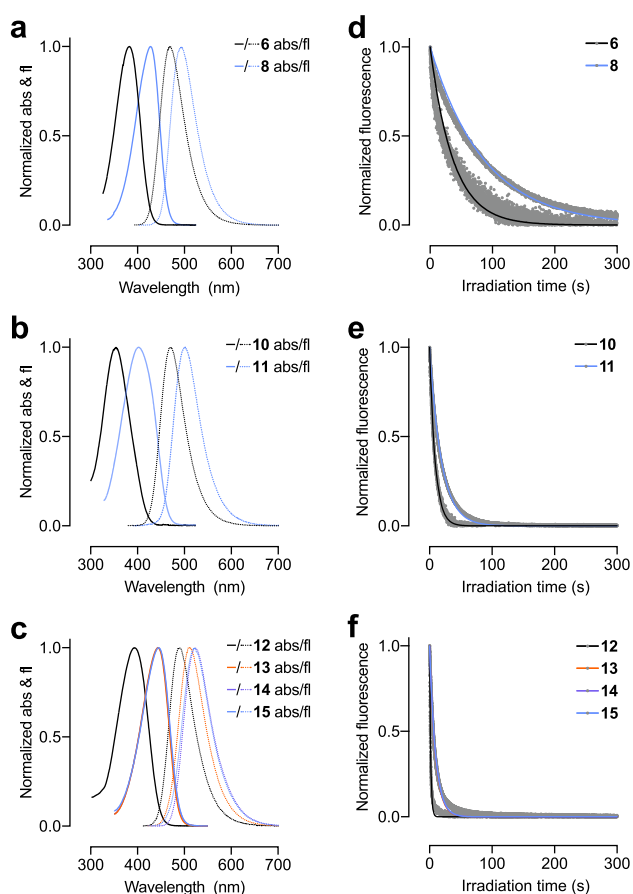
Figure 2. Spectra and photobleaching of representative DAB dyes. (a−c) Normalized absorption (abs) and fluorescence emission (fl) of (a) **6** and **8**, (b) **10** and **11**, and (c) **12−15**. (d−f) Plot of normalized fluorescence vs irradiation time of (d) **6** and **8**, (e) **10** and **11**, and (f) **12−15** with monoexponential fit.

dyes **13−15** derived from Coumarin 102 (**12**), the λ_{abs} does not depend on the different secondary amine auxochromes (Table 1, Figure 2c). The fluorescence emission does vary with structure; the acyclic *N,N*-diethylamino derivative **13** exhibits λ_{em} = 513 nm, which is 10 nm shorter than **14** and **15**, resulting in a smaller Stokes shift of 68 nm.

Across the series, we found that the absorptivity of the DAB dyes is substantially higher than the parent coumarin fluorophores, with 1.5−2-fold increases in extinction coefficient at λ_{abs} (ε, Table 1). The transformation of the coumarin oxygen into an iminium moiety elicits variable effects on fluorescence quantum yield (Φ_f). For the relatively dim Coumarin 1 (**6**; Φ_f = 0.06) conversion to DAB dye **8** increases quantum yield (Φ_f = 0.16). In contrast, diazetidinyl dye **11** shows a modestly lower quantum yield (Φ_f = 0.79) compared to the bright azetidinyl coumarin **10** (Φ_f = 0.96). The DAB dyes **13−15** exhibit lower Φ_f values compared to **12**. These modest decreases in Φ_f for compounds **11** and **13−15** are balanced by the larger ε values, resulting in higher molecular brightness ($\varepsilon \times \Phi_f$) for the DAB dyes relative to the corresponding coumarins.

As mentioned above, the DAB dyes exhibit increased photostability compared to their coumarin congeners. Dyes **8** and **11** gave 1.5−2-fold longer t_b values compared to coumarins **6** and **10** (Table 1, Figure 2d,e). For compounds **13−15**, the photostability improvement is greater, with these

DAB compounds showing consistent t_b values that are 5-fold higher than the parent coumarin **12** (Table 1, Figure 2d). Since photobleaching reactions stem from excited states, it is difficult to compare photobleaching time constants between dyes with different fluorescence quantum yields and lifetimes; this is reflected in the different bleaching rates observed across the various dye types (Table 1, Figure 2d−f). We therefore calculated the average total photons (N_p) emitted by each dye.[19] This parameter highlights the increased photostability of the DAB fluorophores and revealed remarkably consistent photostability for compounds **11** and **13−15** with an average of ∼8300 photons/dye (Table 1).

We then evaluated the stability of the iminium linkage in aqueous solution under "dark" conditions and under illumination with violet (405 nm) light. Monitoring with tandem liquid chromatography−mass spectrometry (LC−MS) revealed that all the DAB dyes (**8**, **11**, and **13−15**) show excellent stability with minimal iminium hydrolysis after 48 h at pH 7.4 in the absence of light (Figure 3a,b, Figure S1). We also evaluated the stability of dye **15** in different buffer conditions, observing modestly higher rates of hydrolysis at elevated pH or in cell culture media containing serum (Figure S2). We then undertook a comprehensive photochemistry study of **15** using 405 nm illumination and analysis by LC−MS (Figure 3c,d, Figure S3) The photochemical reactions of **15**
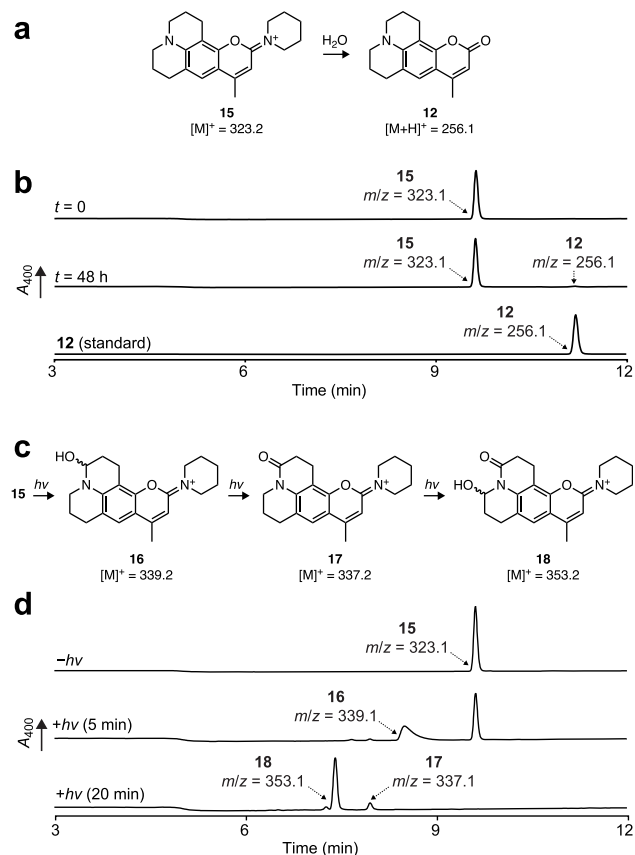

Figure 3. Stability of DAB dye **15**. (a) Spontaneous hydrolysis of **15** to form coumarin **12**. (b) LC−MS chromatograms of **15** at *t* = 0 (top), **15** at *t* = 48 h (middle), and standard **12** (bottom) in PBS, pH 7.4. (c) Photochemistry of **15** to form oxidized adducts **16−18**. (d) LC−MS chromatograms in PBS, pH 7.4, of **15** in the absence of light (top), **15** after 5 min illumination with 405 nm light (middle), and **15** after 20 min illumination with 405 nm light (bottom).

are similar to those observed with parent coumarin 12 where oxidation appears to be centered on the julolidine ring system;[20,21] we did not detect any photochemically driven oxidation on the piperidine ring. Overall, these data show that the DAB dyes exhibit reasonable chemical stability and the iminium motif is not susceptible to photochemical degradation.

Given the propensity of cationic rhodamines to accumulate in the mitochondria (Figure 1a), we investigated the similarly charged DAB dyes as live-cell mitochondrial stains. We incubated live U2OS cells with dyes 8, 11, and 13−15 at 200 nM and co-stained the mitochondria either using MitoTracker Deep Red (Figure 4) or by transient transfection
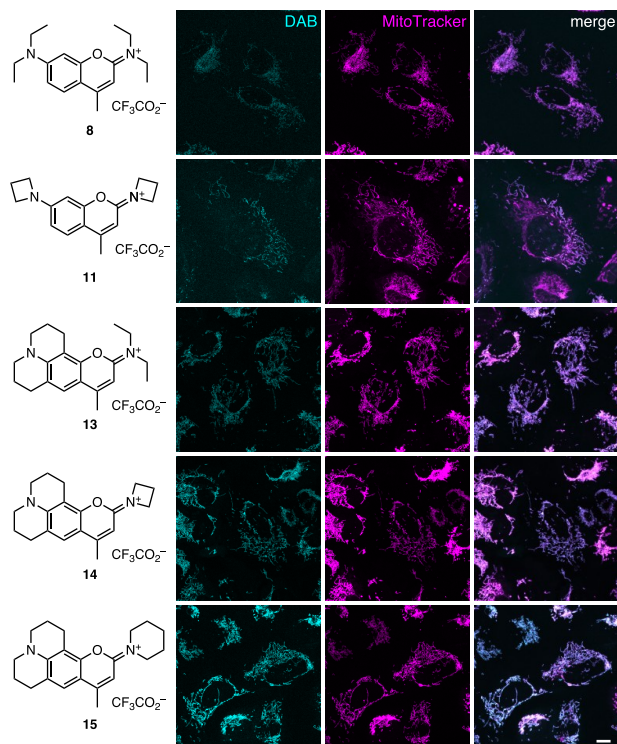

Figure 4. DAB dyes stain mitochondria. Chemical structures of DAB dyes 8, 11, and 13−15 and corresponding fluorescence images of U2OS cells co-stained with the DAB dye (200 nM) and MitoTracker Deep Red (100 nM). Scale bar, 10 μm.

of HaloTag−TOMM20 and staining with the far-red fluorogenic label Janelia Fluor 635-HaloTag ligand[22] (Figure S4). In both experiments, we observed similar staining patterns between the DAB dyes and the established far-red stain or genetically encoded label, confirming our hypothesis that this positively charged fluorophore scaffold would accumulate in mitochondria. Imaging using the same settings revealed that the julolidine-containing derivatives 13−15 showed brighter staining, perhaps due to increased lipophilicity of the compact cationic structure.

In these cellular imaging experiments, we noted that the cellular intensity of even the best DAB mitochondrial stain 15 rapidly decreased upon media exchange. To further improve this reagent, we prepared a dimer derivative of this molecule by reacting Coumarin 102 (12) with dipiperidine 19 to yield "diDAB" 20 (Figure 5a). This design is predicated on two concepts. First, the relatively long Stokes shift of the parent dye 15 (Table 1, Figure 2c) should minimize FRET between the

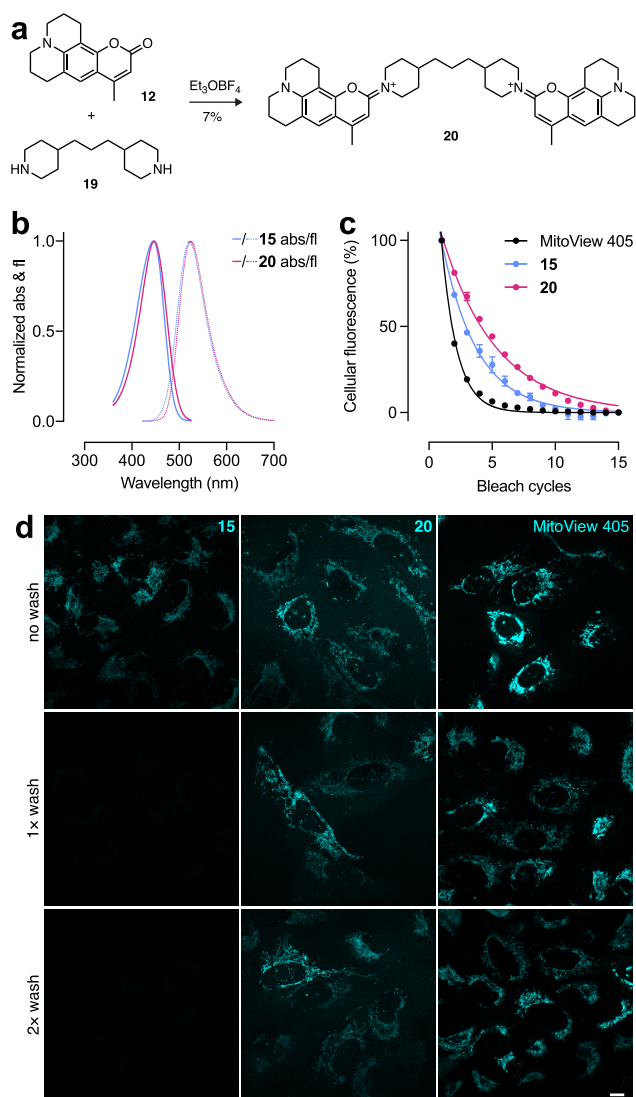**Figure 5.** Dimerization of DAB dye 15 improves performance as a mitochondrial stain. (a) Synthesis of diDAB 20. (b) Normalized absorption (abs) and fluorescence emission (fl) of 15 and 20. (c) Plot of cellular fluorescence vs time of cells incubated with 15, 20, or MitoView 405 during photobleaching; error bars indicate SEM. (d) Live U2OS cells incubated with DAB 15 (200 nM), diDAB 20 (200 nM), or MitoView 405 (100 nM) after 0, 1, or 2 dye-free media exchange washes. Scale bar, 10 μm.

two fluorophore units and preserve fluorescence quantum yield. Second, the presence of two cationic moieties per molecule of 20 should improve mitochondrial retention. Examination of the chemical properties of 20 revealed a slightly higher rate of hydrolysis relative to 15 in different pH conditions even when considering the presence of two iminium groups (Figure S5).

We then measured the spectral properties of the dye dimer. Compound 20 exhibited similar absorption (λ_{abs} = 447 nm) and fluorescence emission (λ_{em} = 524 nm) spectra compared to DAB monomer 15 (Figure 5b); both dyes showed a linear relationship between absorption and concentration ≤20 μM (Figure S6). In aqueous solution, the diDAB 20 did not show the expected 2-fold increase in absorptivity but exhibited ε = 45 200 M^{-1} cm^{-1} along with a modestly lower Φ_f = 0.45 (Table S1). To reconcile this observation and mimic the

nonpolar environment of the mitochondrial inner membrane, we measured the spectral properties of compounds **15** and **20** in sodium dodecyl sulfate (SDS) micelles and dioxane/water mixtures (Table S1). We observed the expected higher ε = 78 900 M^{-1} cm^{-1} in PBS containing 0.1% w/v SDS along with a larger Φ_f = 0.83; compound **20** is also brighter in aqueous dioxane. Although dye **15** also showed higher absorptivity and fluorescence quantum yield in these nonpolar conditions relative to PBS, the effect was less pronounced. We postulate that the relatively low ε and Φ_f observed for compound **20** in aqueous solution is due, in part, to intramolecular interactions between the two chromophore units. These interactions could be reduced in the more hydrophobic environment of SDS micelles or dioxane/water mixtures, resulting in higher absorptivity and fluorescence quantum yield.

We then compared the parent DAB **15**, diDAB **20**, and the commercial violet-excited (and structurally mysterious) MitoView 405 in live-cell experiments. Although MitoView 405 was modestly brighter than DAB **15** or diDAB **20** upon initial application, the dye bleached rapidly in live cells in our hands, preventing acquisition of a full confocal microscopy stack. The DAB compounds exhibited substantially higher resistance to photobleaching with the diDAB **20** showing the best overall photostability (Figure 5c). As expected, all the dyes showed excellent mitochondrial staining upon initial application (Figure 5d). Upon media exchange, however, the DAB **15** signal rapidly decreased whereas the diDAB **20** and MitoView 405 were retained after this cell washing protocol.

CONCLUSION

In summary, we demonstrate that the 2,7-diaminobenzopyrylium (DAB) framework is a modular scaffold for the synthesis of mitochondrial stains excited with violet light. These atom-efficient imaging reagents can be prepared from the broad palette of 7-aminocoumarin dyes with different N-substitution patterns (Scheme 1). Although the spectral properties can be tuned by choosing different coumarin starting materials, the structure of the secondary amine reactant has only minor effects on the properties of the resulting DAB dyes: use of azetidine or piperidine gave fluorophores with similar quantum yields and photostability (Table 1). This is in contrast to rhodamine dyes, where azetidine or piperidine auxochromes can elicit 10-fold changes in Φ_f.[18] The DAB dyes exhibit higher absorptivity and photostability than their coumarin parent dyes (Table 1, Figure 2), show reasonable chemical stability (Figure 3), and are effective mitochondrial stains (Figure 4); dimerization of the DAB dye affords a stain with better cellular retention (Figure 5). Looking forward, the utility of these bright, photostable, and biocompatible "mini-rhodamines" (Figure 1) could be expanded beyond mitochondrial stains. The stability of the iminium moiety could be improved through intramolecular cyclization to develop new conjugatable fluorescent labels or photolabile groups. The slow rate of hydrolysis could also be tuned and exploited to release coumarin-based drugs.[23] Overall, the DAB dyes represent an underutilized chemical scaffold worthy of further attention.

ASSOCIATED CONTENT

S1 Supporting Information

The Supporting Information is available free of charge at https://pubs.acs.org/doi/10.1021/acsbiomedchemau.1c00068.

Chemical stability of dyes in PBS, stability of **15** under different conditions, photochemistry of **15**, mitochondrial staining with DAB dyes, comparison of stability of **15** and **20**, Beer−Lambert−Bouguer analysis of **15** and **20**, spectral properties of **15** and **20** in different solvents, spectroscopy and imaging experimental details, synthetic organic chemistry details, and characterization of novel compounds (PDF)

AUTHOR INFORMATION

Corresponding Author

Luke D. Lavis − *Janelia Research Campus, Howard Hughes Medical Institute, Ashburn, Virginia 20147, United States;* orcid.org/0000-0002-0789-6343; Email: lavisl@ janelia.hhmi.org

Authors

Sambashiva Banala − *Janelia Research Campus, Howard Hughes Medical Institute, Ashburn, Virginia 20147, United States*

Ariana N. Tkachuk − *Janelia Research Campus, Howard Hughes Medical Institute, Ashburn, Virginia 20147, United States*

Ronak Patel − *Janelia Research Campus, Howard Hughes Medical Institute, Ashburn, Virginia 20147, United States*

Pratik Kumar − *Janelia Research Campus, Howard Hughes Medical Institute, Ashburn, Virginia 20147, United States*

Timothy A. Brown − *Janelia Research Campus, Howard Hughes Medical Institute, Ashburn, Virginia 20147, United States*

Complete contact information is available at:
https://pubs.acs.org/10.1021/acsbiomedchemau.1c00068

REFERENCES

(1) Crivat, G.; Taraska, J. W. Imaging proteins inside cells with fluorescent tags. *Trends Biotechnol.* **2012**, *30*, 8−16.

(2) Bruchez, M. P. Dark dyes-bright complexes: Fluorogenic protein labeling. *Curr. Opin. Chem. Biol.* **2015**, *27*, 18−23.

(3) Lavis, L. D. Chemistry is dead. Long live chemistry! *Biochemistry* **2017**, *56*, 5165−5170.

(4) Erdmann, R. S.; Baguley, S. W.; Richens, J. H.; Wissner, R. F.; Xi, Z.; Allgeyer, E. S.; Zhong, S.; Thompson, A. D.; Lowe, N.; Butler, R.; Bewersdorf, J.; Rothman, J. E.; St Johnston, D.; Schepartz, A.; Toomre, D. Labeling strategies matter for super-resolution microscopy: A comparison between HaloTags and SNAP-tags. *Cell Chem. Biol.* **2019**, *26*, 584−592.

(5) Grimm, J. B.; Lavis, L. D. Caveat fluorophore: An insiders' guide to small-molecule fluorescent labels. *Nat. Methods* **2022**, *19*, 149.

(6) Valm, A. M.; Cohen, S.; Legant, W. R.; Melunis, J.; Hershberg, U.; Wait, E.; Cohen, A. R.; Davidson, M. W.; Betzig, E.; Lippincott-Schwartz, J. Applying systems-level spectral imaging and analysis to reveal the organelle interactome. *Nature* **2017**, *546*, 162−167.

(7) Haugland, R. P.; Spence, M. T. Z.; Johnson, I. D.; Basey, A. *The handbook: A guide to fluorescent probes and labeling technologies*, 10th ed.; Molecular Probes: Eugene, OR, 2005.

(8) Dolman, N. J.; Kilgore, J. A.; Davidson, M. W. A review of reagents for fluorescence microscopy of cellular compartments and structures, Part I: BacMam labeling and reagents for vesicular structures. *Curr. Protoc. Cytom.* **2013**, *65*, 12.30.1−12.30.27.

(9) Foster, T. P. Probes for fluorescent visualization of specific cellular organelles. In *Immunohistochemistry and Immunocytochemistry: Methods and Protocols*; Del Valle, L., Ed.; Springer US: New York, NY, 2022; pp 85−124.

(10) Pierzynska-Mach, A.; Janowski, P. A.; Dobrucki, J. W. Evaluation of acridine orange, LysoTracker Red, and quinacrine as fluorescent probes for long-term tracking of acidic vesicles. *Cytometry A* **2014**, *85*, 729−737.

(11) Greenspan, P.; Mayer, E. P.; Fowler, S. D. Nile Red: A selective fluorescent stain for intracellular lipid droplets. *J. Cell Biol.* **1985**, *100*, 965−973.

(12) Johnson, L. V.; Walsh, M. L.; Chen, L. B. Localization of mitochondria in living cells with rhodamine 123. *Proc. Natl. Acad. Sci. U. S. A.* **1980**, *77*, 990−994.

(13) Scaduto, R. C., Jr.; Grotyohann, L. W. Measurement of mitochondrial membrane potential using fluorescent rhodamine derivatives. *Biophys. J.* **1999**, *76*, 469−477.

(14) Haugland, R. P.; Johnson, I. D. Detecting enzymes in living cells using fluorogenic substrates. *J. Fluoresc.* **1993**, *3*, 119−127.

(15) Huang, S.-T.; Jian, J.-L.; Peng, H.-Z.; Wang, K.-L.; Lin, C.-M.; Huang, C.-H.; Yang, T. C. K. The synthesis and optical characterization of novel iminocoumarin derivatives. *Dyes Pigm.* **2010**, *86*, 6−14.

(16) Liepouri, F.; Foukaraki, E.; Deligeorgiev, T. G.; Katerinopoulos, H. E. Iminocoumarin-based low affinity fluorescent Ca2+ indicators excited with visible light. *Cell Calcium* **2001**, *30*, 331−335.

(17) Kirpichenok, M. A.; Gorozhankin, S. K.; Yufit, D. S.; Struchkov, Y. T.; Kurapov, P. B.; Grandberg, I. I. Synthesis and spectral-luminescent properties of 2,7-diaminobenzopyrylium tetrafluoroborates. *Khim. Geterotsikl. Soedin.* **1989**, *6*, 755−766.

(18) Grimm, J. B.; English, B. P.; Chen, J.; Slaughter, J. P.; Zhang, Z.; Revyakin, A.; Patel, R.; Macklin, J. J.; Normanno, D.; Singer, R. H.; Lionnet, T.; Lavis, L. D. A general method to improve fluorophores for live-cell and single-molecule microscopy. *Nat. Methods* **2015**, *12*, 244−250.

(19) Abdelfattah, A. S.; Kawashima, T.; Singh, A.; Novak, O.; Liu, H.; Shuai, Y.; Huang, Y. C.; Campagnola, L.; Seeman, S. C.; Yu, J.; Zheng, J.; Grimm, J. B.; Patel, R.; Friedrich, J.; Mensh, B. D.; Paninski, L.; Macklin, J. J.; Murphy, G. J.; Podgorski, K.; Lin, B. J.; Chen, T. W.; Turner, G. C.; Liu, Z.; Koyama, M.; Svoboda, K.; Ahrens, M. B.; Lavis, L. D.; Schreiter, E. R. Bright and photostable chemigenetic indicators for extended in vivo voltage imaging. *Science* **2019**, *365*, 699−704.

(20) Kuznetsova, N. y. A.; Kaliya, O. L. The photochemistry of coumarins. *Russ. Chem. Rev.* **1992**, *61*, 683−696.

(21) Zheng, Q.; Lavis, L. D. Development of photostable fluorophores for molecular imaging. *Curr. Opin. Chem. Biol.* **2017**, *39*, 32−38.

(22) Grimm, J. B.; Muthusamy, A. K.; Liang, Y.; Brown, T. A.; Lemon, W. C.; Patel, R.; Lu, R.; Macklin, J. J.; Keller, P. J.; Ji, N.; Lavis, L. D. A general method to fine-tune fluorophores for live-cell and in vivo imaging. *Nat. Methods* **2017**, *14*, 987−994.

(23) Stefanachi, A.; Leonetti, F.; Pisani, L.; Catto, M.; Carotti, A. Coumarin: A natural, privileged and versatile scaffold for bioactive compounds. *Molecules* **2018**, *23*, 250.